Global J. Environ. Sci. Manage. 7(4): 625-642, Autumn 2021

Global Journal of Environmental Science and Management
(GJESM)

Homepage: https://www.gjesm.net/

ORIGINAL RESEARCH PAPER

Characteristics and combustion kinetics of fuel pellets composed of waste of polyethylene terephthalate and biomass

K. Manatura[1], U. Samaksaman[2,*]

[1]*Department of Mechanical Engineering, Faculty of Engineering at Kamphaeng Saen, Kasetsart University, Kamphaeng Saen campus, Nakhonpatom, Thailand*

[2]*Department of Natural Resources and Environment, Faculty of Agriculture Natural Resources and Environment, Naresuan University, Phitsanulok, Thailand*

ARTICLE INFO

Article History:
Received 02 February 2021
Revised 21 April 2021
Accepted 22 May 2021

Keywords:
Biomass
Characteristics
Combustion
Kinetics
Pellets
Polyethylene terephthalate (PET)
Thermogravimetric analyzer (TGA)

ABSTRACT

BACKGROUND AND OBJECTIVES: The needs of fuel pellets from varied feed stocks have opened up opportunities and challenges for pellets production from non-woody biomass. Wastes of plastic recycling and wood sawing contained a high potential for energy source and suited for pelletizing as a solid fuel.

METHODS: The characteristics and combustion kinetics of fuel pellets made using a mixture of waste of polyethylene terephthalate and biomass (Tectona grandis Linn.f) with a polyethylene terephthalate to biomass ratio of 9:1. The investigation covered physico-chemical properties and their functional group analysis, heavy metal concentration and ionic leachability testing, and ash analysis. In this context, thermogravimetric analysis was used in an atmosphere of oxygen gas, over a temperature range of 50-800 °C and at different heating rates. The work ends with discussion of the kinetics study via three comparative evaluations and the feasibility of fuel pellets for energy utilization.

FINDINGS: Pelletizing with this ratio (9:1) was present the durability of PET/biomass pellets, a uniform dimension, ease handling, storage, and transportation common as woody pellets. Some technical challenges such as low moisture content and high volatile matter content were feedstock dependent. The major characteristics were a combination of those from both the constituent materials. Functional groups of the pellets were contributed by terephthalate and lignocellulose. The addition of a small amount of biomass in pellets could improve their thermal decomposition behavior. The properties of the polyethylene terephthalate/biomass pellets indicated that were fit for combustion with a high heating value equal to 19.20 MJ/kg. Heavy metals and ionic contaminants were below the maximum limits of the standards because of the cleanliness of the raw materials. However, the minor effects of earth materials and a caustic soda detergent were resulted in the alteration of residue chemicals. The pellets had lower ignition, devolatilization, and burnout temperatures than the original polyethylene terephthalate waste; likewise, the peak and burnout temperatures shifted to a lower zone. The activation energy values obtained using the Kissinger-Akahira-Sunose, Ozawa-Flynn-Wall, and Starink models were similar and in the range 142–146 kJ/mol.

CONCLUSION: These findings may provide crucial information on fuel pellets from blended polyethylene terephthalate/biomass to assist the design and operation of a co-combustion system with traditional solid fuels. Such modifications of fuel pellets suggest the possibility of operating in large-scale furnace applications and can further be upgraded to other fuels production via modern bioenergy conversion processes.

DOI: 10.22034/gjesm.2021.04.09

NUMBER OF REFERENCES	NUMBER OF FIGURES	NUMBER OF TABLES
58	6	9

*Corresponding Author:
Email: *ukrits@nu.ac.th*
Phone: +66 5596 2754
Fax: +66 5596 2750

Note: Discussion period for this manuscript open until January 1, 2022 on GJESM website at the "Show Article.

INTRODUCTION

The use of plastics has increased tremendously around the world due to their compatible properties in diversified applications, as well as being relatively cheap and safe. Post-consumption plastic is regarded as a major waste source and creates unhealthy conditions for humans and the environment (Patnaik *et al.,* 2020). The ever-rising amount of plastic waste has tended to increase polyethylene terephthalate (PET) waste. PET usage has rapidly grown in daily life applications such as bottling carbonated soft drinks, beverages, and other liquids and as food containers, microwave trays, and food packaging films. Furthermore, it is appropriate for lightweight, large-capacity, and shatter-resistant containers which are mainly found in the shipping industry (Sinha *et al.,* 2010). Used PET bottles can be recycled using a mechanical recycling process that uses shredding and crushing to convert a bottle into flakes (Jabłońska *et al.,* 2019). In this process, purification and decontamination of the PET-flake are important methods followed by washing (with a detergent) and water soaking, centrifuging, drying, and separating foreign plastics. PET-flake from these processes can be utilized as raw-PET for producing goods with both up- and down-cycling processes (Tolinski, 2011). Nevertheless, secondary waste from a mechanical recycling plant occurs as the process releases undesired materials such as dust, sludge, debris, tiny pieces, and microplastics, as mentioned waste of PET. These amount to 3-5% by weight (%wt) of the PET bottle in a mechanical recycling plant and it is feasible to recover energy and importantly reduce the amount of waste landfill (Beata *et al.,* 2019; Surenderan *et al.,* 2018). Biomass is considered one of the most important renewable sources and is produced in large amounts in industry, agriculture, and forestry (Becidan *et al.,* 2007). It can be directly used or used cooperatively with coal and other solid fuels (Ahn *et al.,* 2014; Basu *et al.,* 2011; Nussbaumer, 2003; Sajdak *et al.,* 2019). Teak sawdust (*Tectona grandis* Linn.f) provides as a waste of wood industry in the sub-regional area of northern Thailand. It is used as a fuel for firing in pottery furnaces and biomass power plants. Furthermore, it is used as a mixture material for mushroom and vegetable plantation. Pelletizing is one process for handling powder-like materials such as dust, sludge, debris, tiny pieces, and microplastic as well as biomass and sawdust to become fuel pellets. Moreover, it has been widely used for mass and energy densification to overcome the disadvantages associated with raw material use (Mostafa *et al.,* 2019). To avoid the resource wastage and environment contamination, fuel pellets production is proposed to utilize the waste of PET and biomass. Currently, waste of PET and teak sawdust for alternative use is mainly received from local factories. Efforts are being made to understand as the study novelty in the co-densification of the mixtures of dusty PET waste and sawdust invite new chalanges to pelletization process. In addition, the detailed studies of fuel pellets from varied feedstocks with different morphology and characteristics are opened up opportunities and challenges (Pradhan *et al.,* 2018). Thus, the co-densification of waste of PET and teak sawdust can be discussed. The use of this type of fuel in co-firing processes reduces greenhouse gas emission and cheaper than traditional fuels (coal, lignite) and sometimes get income by a surcharge (Jabłońska *et al.,* 2019). Previous works, the pyrolysis-gasification of biomass/PET feedstock has been extensively studied by numerous researchers (Abnisa and Wan Daud, 2014; Bu *et al.,* 2018; Madadian *et al.,* 2017; Narobe *et al.,* 2014; Robinson *et al.,* 2016). They reported that the composition and fraction of the feedstock have an important influence on the distribution, composition, and characteristics of the gas, liquid, and solids (Block *et al.,* 2019; Çepelioğullar and Pütün, 2013). Chattopadhyay *et al.* (2009), reported a significant interaction or synergistic effect between plastics and biomass (paper) under pyrolysis in a thermogravimetric analyzer (TGA). Paper-biomass started to decompose at a lower temperature (below 100 °C) than plastics and rapidly degraded at 350 °C. At higher temperature, PET started with an initial degradation temperature of 200 °C followed by a curve of rapid degradation at around 420-490 °C and a small amount at around 500-550 °C. Since the chemicals in plastic easily break up at higher temperatures, increased mass loss is observed more rapidly at a high temperature. Plastics/biomass composited with a mixed plastics (HDPE, PP, PET) to biomass ratio of 9:1 had the best performance with a slightly decreased mass loss during thermal degradation of 5% at a lower temperature and significantly decreased mass loss of over 95% at 500 °C. This may be due to the higher ratio of plastic in the mixture contains lower moisture, ash, and fixed

carbon contents than for a low ratio of plastics in fuel pellets (Martín-Gullón *et al.,* 2001). Energy required for the pyrolysis of multicomponent mixtures of waste PET and solid biomass increased with increase in amount of plastic content in the mixture due to the pyrolysis of PET plastic needs more energy than wood (Wang *et al.,* 2021). Combustion of multicomponent mixtures acquired lower the activation energy than pyrolysis, therefore the leads of a minimum biomass supplied as part of plastic wastes instead of a minimum plastic waste supplied as part of biomass needs to be examined further. It is noticed that the study in fraction of these materials (PET/biomass) has not fully explored. The approach has to account for the behavior of PET/biomass during combustion. TGA is a worldwide method to analysis thermal behavior of materials such as food, feedstock, chemical, soil, fertilizer, plastic, advance polymers, biomass, solid fuels such as coal, lignite, shale oil, and so on. TGA is one of the most extensive practices for the preliminary prediction of thermal behavior and kinetics for complex solid fuels (Govindan *et al.,* 2018; Yuan *et al.,* 2017). In TGA, the thermal decomposition of the sample under a selective environment is analyzed by determining its mass loss during an increased temperature duration (Chandrasekaran *et al.,* 2017; Xie *et al.,* 2019). The mass loss is used to determine kinetic parameters including the activation energy, pre-exponential factor, and reaction mechanism. Two common approaches applied for kinetic analysis are the model-fitting and model-free (iso-conversional) methods. The analysis is accurate and convenient for iso-conversional methods compared to model-fitting methods (Bu *et al.,* 2018). Only few data on heating rates assuming negligible mass transfer are required to estimate the activation energy in terms of the degree of conversion (Vyazovkin and Wight, 1999; Xu and Chen, 2013). Many iso-conversional methods, such as the Friedman, Ozawa-Flynn-Wall (OFW), Kissinger-Akahira-Sunose (KAS), and Starink methods have been used for the kinetic analysis of oxidative and non-oxidative processes in various types of solid fuels, including coal and biomass (Chen *et al*., 2017; Sharara and Sadaka, 2014; Slopiecka *et al.,* 2012). There is a need for research into the utilization of waste of PET by pelletizing in combination with local biomass that could be applied in process of waste to energy. It is a new study pathway revealed with the novel materials, techniques of analysis, and evaluation. The important properties and crucial data of characteristics of fuel pellets from blended PET/biomass with a view towards energy recovery in the combustion process are also considered. Moreover, this study aims to determine their functional group, heavy metals and ionic contaminants, and residue composition as well as evaluation of the kinetic parameters by iso-conversional methods (OFW, KAS, and Starink methods). It is expected that the knowledge of the characteristics and combustion behavior of the PET/biomass pellets and in particular the precise estimation of kinetics, will provide essential guidance for further work. This study has been carried out in Phitsanulok province, Thailand in 2019.

MATERIALS AND METHODS

Raw materials and pelletizing

The waste of PET was sourced from a bulk of waste plastics at a PET bottle recycling plant in Surin province, Thailand. The similar case of mechanical recycling processes for used PET bottles was demonstrated by Jabłońska *et al.* (2019). The sample of PET waste contained different sizes of PET plastic from <0.5 to 1.5 mm (sieve size no. 14-35). Biomass (teak sawdust; *Tectona grandis* Linn.f) was sourced from a saw mill in Phrae province, Thailand. Both the PET waste and biomass were dried before pellet production. The fuel pellets of PET/biomass was produced using a flat-die pelletizing machine. Prior to pelletizing, the machine was warmed using a mixture of PET/biomass as a pre-pelleting material. Then, the mixture of PET and biomass (9:1, w/w) was fed at a continuous rate of 1 kg/min. About 10%wt of water was added during the process to prevent materials from sticking. Pellets were approximately 1.0 cm in diameter and 2.4 cm in length, as shown in Fig. 1. Then, pellets were dried in an air oven at 65 °C for 12 hours.

Proximate, ultimate, and calorific value tests

The samples of PET waste, biomass, and PET/biomass pellets were analyzed to determine their physical and chemical properties with three replications. The moisture content (MC) was measured by weighting mass before and after heat in a hot-air oven at 105 °C for 24 hours. Volatile matter (VM) of sample was measured by weighting mass before and after the covered sample-containing crucible in



Fig. 1: A flat-die pelletizing machine and the PET/biomass pellets

a muffle furnace at 900±10 °C for 4 minutes (CEN/TS 15148). The sample in uncovered crucible was heated at 550±10 °C for 2 hours to determine the ash content (CEN/TS 14775). The fixed carbon (FC) was found by subtraction; FC = 100 - (MC + VM + ash). The carbon (C), hydrogen (H), nitrogen (N), and sulfur (S) contents of samples were determined using a TrueSpec Micro (Leco, CHNS628) and the oxygen (O) content was calculated based on dry ash-free basis by using the formula; O = 100 - (C + H + N + S + ash), more details found as Samaksaman *et al.* (2021). In addition, the high heating value (HHV) was carried out based on analysis of the calorific value using a bomb calorimeter (Leco, AC-500) in an atmosphere of oxygen.

Fourier transform infrared spectrometry (FTIR)

Raw materials and PET/biomass pellets were tested for the determination of the functional groups of polyethylene terephthalate (polyester group) and biomass components (lignocellulose group) using FTIR technique (Perkin Elmer, Spectrum GX). The IR spectra were recorded at wavenumbers in the range 4,000 to 400/cm at a resolution of 1/cm. The data were interpreted using the Perkin Elmer Spectrum version 10.5.2 software.

Heavy metal and ionic leachability tests

The PET waste and biomass may become contaminated with heavy metals and minerals during the process of mechanical recycling and sawing. These metals may cause scratching and corrosion of machinery. Heavy metals concentration such as copper (Cu), zinc (Zn), chromium (Cr), cadmium (Cd), and lead (Pb) were investigated. The procedure was detailed in a previous work of Samaksaman *et al.* (2015). Samples of PET waste, biomass, and PET/biomass pellets were digested using an acidic solution (a mixture of hydrochloric and nitric acids), followed by dilution with deionized (DI) water and filtration. Atomic absorption spectrometry (GBC, Avanta PM) was used in the subsequent analysis. The standardized curves with coefficient of determination (R^2) values of 0.95-0.99 were used to evaluate heavy metal concentrations. The leachability test was used to determine the concentration of ionic leachates from the samples. The test applies quantity analysis of elements for seven anions leachate (AnL): fluoride (F^-), chloride (Cl^-), nitrite (NO_2^-), bromide (Br^-), nitrate (NO_3^-), phosphate (PO_4^{3-}), and sulfate (SO_4^{2-}); and for six cations leachate (CaL): lithium (Li^+), sodium (Na^+), ammonium (NH_4^+), potassium (K^+), magnesium (Mg^{2+}), and calcium (Ca^{2+}). One gram of each sample

was placed in a centrifuge tube and mixed with 10 ml DI water. A shaking incubator (JSR, Jssi-300C) was used for extraction at 250 rpm at room temperature for 12 hours. Then the sample was filtered twice using a paper filter before passing through a nylon filter. Prior to measurement, dilution of the sample (1:100 v/v) with ≥18 (mΩ) DI water was carefully conducted in a clean room. The sample solution was analyzed for anions and cations using ion chromatography (Dionex DX500). All experiments were done three replications.

Ash composition analysis

X-ray fluorescence (XRF) spectroscopy is a rapid method used to determine the composition in solid samples like ash and residue. It is a non-destructive technique and suitable for ash samples from the combustion test. The ash samples were the as-receive samples from the combustion of raw materials and pellets within a muffle furnace at 815 °C for 2 hours (Xing *et al.,* 2016). The test was employed using an energy dispersive XRF (EDXRF, Horiba XGT-5200 X-ray Analytical Microscope) with Rh X-ray tube, 1.2 mm of XGT diameter, and 30 kV of X-ray tube voltage.

Thermogravimetric analysis

A simultaneous thermal analyzer (Mettler-Toledo, TGA-DSC II) was used to measure the thermal decomposition of samples. Thermogravimetric analysis and derivative thermogravimetry (DTG) were used to analyze samples of PET waste, biomass, and PET/biomass pellets. Raw materials were analyzed in an atmosphere of oxygen, over a temperature range of 50-800 °C at a heating rate of 15 °C/min. The PET/biomass pellets were analyzed under the same conditions as the raw materials but various heating rates of 5, 10, 15, and 20 °C/min.

Kinetic analysis

The combustion of carbonaceous material is considered in term of a gas-solid heterogeneous reaction. The conversion (X) of PET waste, biomass, and pellets during the combustion process can be defined using Eq. 1.

$$X = \frac{m_0 - m_t}{m_0 - m_f} \quad (1)$$

Where, m_0, m_t, and m_f are the initial sample mass, the sample mass at time *t*, and the sample mass left after ending process, respectively. The combustion rate of the materials can be represented using Eq. 2.

$$\frac{dX}{dt} = k(T) f(X) \quad (2)$$

Where, *k* is the combustion rate constant and *f(x)* is the reaction model expressing the dependence of the combustion rate. The combustion rate constant *(k)* is temperature-dependent and generally is described using the Arrhenius formula using Eq. 3 (Mishra *et al.,* 2019).

$$k = Ae^{-E_a/RT} \quad (3)$$

Where, E_a is the activation energy (kJ/mol), A is the pre-exponential factor (s^{-1}), T is the absolute temperature (K), and R is the universal gas constant, 8.314 kJ/(kmol·K). A heterogeneous function of the uniform kinetic reaction of the first order (n = 1), *f(x)* can be written using Eq. 4.

$$f(X) = (1 - X) \quad (4)$$

Thus, the rate constant can be expanded using Eq. 5.

$$\frac{dX}{dt} = Ae^{-E/RT}(1 - X) \quad (5)$$

In non-isothermal analysis, the heating rate varies with the reaction time and temperature at a constant heating rate, $\beta = \frac{dT}{dt}$ that can be rewritten as Eq. 6.

$$\frac{dX}{dT} = \frac{A}{\beta} e^{-E/RT}(1 - X) \quad (6)$$

The integral form of *f(X)* can be represented as g*(X)* by integrating Eq. (6) with respect to temperature as shown in Eqs. 7 and 8.

$$g(X) = \int_0^X \frac{dX}{f(X)} = \frac{A}{\beta} \int_{T_0}^{T} e^{-E/RT} dT \quad (7)$$

$$g(X) = \frac{AE}{\beta R} \int_0^X u^{-2} e^{-u} du = \frac{AE}{\beta R} p(X) \quad (8)$$

Kissinger-Akahira-Sunose method

The Kissinger-Akahira-Sunose (KAS) method (Akahira and Sunose, 1971) is an iso-conversional method that uses an approximation of $p(X) = x^{-2}e^{-x}$ in Eq. (8) to determine E_a as shown in Eq. 9.

$$\ln\left(\frac{\beta}{T^2}\right)=\ln\left(\frac{AE_a}{Rg(X)}\right)-\left(\frac{E_a}{RT}\right) \quad (9)$$

Plotting $\ln\left(\frac{\beta}{T^2}\right)$ versus 1/T will obtain the slope and intercept that can be used to estimate E_a and A, respectively.

Ozawa-Flynn-Wall method

The Ozawa-Flynn-Wall (OFW) method is a model-free method applying Doyle's approximation in Eq. (8) to evaluate the activation energy (Tran *et al.,* 2014) as shown in Eq. 10.

$$\ln(\beta)=\ln\left(\frac{AE_a}{Rg(X)}\right)-5.3305-1.052\left(\frac{E_a}{RT}\right) \quad (10)$$

E_a was determined using the least square regression line as the slope of $1.052E_a/R$ by plotting the graph between ln (β) on the y-axis versus 1/T on the x-axis.

Starink method

The Starink method is a model-free method like the KAS and OFW methods; however, the value it produces for E_a is more accurate than from using the other two methods (Gai *et al.,* 2013). The Starink equation is shown in Eq. 11.

$$\ln\left(\frac{\beta}{T^{1.8}}\right)=C_s-1.0037\left(\frac{E_a}{RT}\right) \quad (11)$$

Plotting a linear graph of $\ln\left(\frac{\beta}{T^{1.8}}\right)$ and 1/T enables the values of E_a and A to be determined from the slope and intercept, respectively.

Thermodynamic analysis

Thermodynamic parameters can be presented by the change in the enthalpy (ΔH), Gibbs free energy (ΔG), and entropy (ΔS) (Manatura, 2019). In brief, ΔH represents an endothermic or exothermic reaction which is the nature of the reaction process. ΔG indicates the energy related to a chemical reaction that can be used to do work and ΔS measures the irreversibility of the system. The parameters can be calculated using Eqs. 12-14.

$$\Delta H=E_a-RT \quad (12)$$

$$\Delta G=E_a+RT_p\ln\left(\frac{K_BT_p}{hA}\right) \quad (13)$$

$$\Delta S=\frac{\Delta H-\Delta G}{T_p} \quad (14)$$

Where, K_B, h, and T_p are the Boltzmann constant = 1.381×10^{-23} J/K, Plank constant = 6.626×10^{-34} J.s and peak temperature, respectively.

RESULTS AND DISCUSSION

Properties and fuel characteristics

Table 1 shows that the proximate and ultimate analysis for entire PET waste, biomass, and PET/biomass pellet samples. The PET waste had lower moisture and ash content compared to the biomass. The PET waste contained large amounts of volatile matter due to the nature of the plastic material (Luo *et al.,* 2018; Zhao *et al.,* 2016). The PET/biomass pellets also contained a large amount of volatile matter (83.19%). However, it had higher ash content (4.62%) and fixed carbon (6.83%) than the biomass. These changes in the physical properties of the pellets were due to the mixing ratio and the pelletizing process. Subsequently, the HHV of pellets was 19.20 MJ/kg via the calorimetric test and was slightly different from the HHV of pellets via calculation (Huang and Lo, 2020). Mass and energy densification by pelletizing could overcome the disadvantages of PET waste and biomass. The H/C and O/C atomic ratios of PET waste, biomass, and pellet samples were in the range of 0.08–0.13 and 0.85–1.47, respectively. The H/C value for the PET waste was different compared to the biomass and was linked to the H/C value of the PET/biomass pellets. The PET/biomass pellets had a

Table 1: Properties of the raw materials and PET/biomass pellets

Sample	Proximate analysis (%wt)				Ultimate analysis (%wt)					H/C	O/C	HHV (MJ/kg)
	MC	VM	FC	Ash	C	H	N	O	S			
PET	5.09	87.80	5.02	2.09	38.41	3.02	0.08	56.40	ND	0.08	1.47	21.77
Biomass	7.78	78.33	8.26	5.63	47.58	6.32	0.06	40.41	ND	0.13	0.85	17.39
Pellets	5.36	83.19	6.83	4.62	39.33	3.35	0.07	49.43	ND	0.09	1.26	19.20

ND: not detected

higher H/C value mainly due to the PET composition. The percentage of N showed similar results in the range 0.06-0.08% for the raw materials, while the percentage of S was untraceable in all samples. Previous works reported that C and H contents in PET samples were higher compared to the current study (Luo *et al.,* 2018; Surenderan *et al.,* 2018; Zhao *et al.,* 2016). The N and S content was substantially low. Low emissions of oxides of nitrogen (NO_x) and sulfurdioxide (SO_2) could be expected when this PET/biomass pellet was used as fuel in the combustion or co-combustion processes (Edo *et al.,* 2016). The current results from the proximate and ultimate analysis suggested that the purity of the PET waste was an important factor in determining their characteristics. Compared to PET waste from bottles, the pure-PET had less contaminants and decay materials from the mechanical process, it would be clearly resulted as a previous work by Jabłońska *et al.* (2019). In the pelletizing of PET waste and biomass into a fuel pellet, the PET plastic played a key role in the compaction and made the pellets harden, as seen in Fig. 1. In conclusion for this sub-section, the PET/biomass pellets could be used as alternative sources and in combination with solid fuels in the same manner as refuse-derived fuel (RDF) and solid recovered fuel (SRF).

FTIR results

The FTIR technique allowed the identification of the functional groups present in the polyethylene terephthalate (polyester group) and biomass components (lignocellulose group). Fig. 2a-c illustrates the IR spectra of samples of PET waste, biomass, and PET/biomass pellets. The identified vibrational groups are summarized in the Table 2. The bands were in agreement with previous works (Chen *et al.,* 2013; Lopes *et al.,* 2018; Manatura, 2020; Pereira *et al.,* 2017; Taleb *et al.,* 2020). The IR spectrum of PET waste (Fig. 2a) contained bands at 2,916/cm (C-H, stretch), 1,714/cm (C=O, stretch), and 1,338-1,408/cm (C-O, stretch). The main observation at 1,247/cm and 1,125/cm affirmed the terephthalate group ($OOCC_6H_4$-COO). The same results for the PET functional groups were suggested by previous researchers (Chen *et al.,* 2013; Pereira *et al.,* 2017). In addition, the IR bands of the PET waste at around 1,090, 950-1,016, 796, and 439/cm, represented groups of Si-O asymmetric, Si-O(H) asymmetric, Si-O symmetric, and Si-O-Si bending, respectively (Capeletti and Zimnoch, 2016; Pereira *et al.,* 2017). These results were due to the characteristics of soil and sand that remained in the PET waste from the mechanical recycling process of the PET bottles. The IR spectrum of the biomass sample in Fig. 2b shows

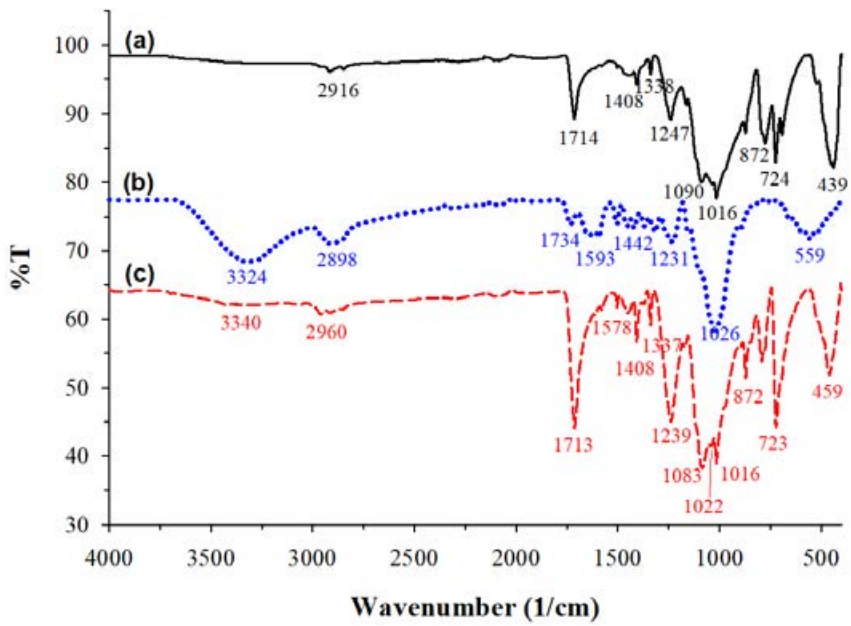


Fig. 2: IR spectra of samples; (a) PET waste, (b) biomass, and (c) PET/biomass pellets

Table 2: Characteristics bands of the PET waste, biomass, and pellets obtained by FTIR

Wavenumber (1/cm)			Characteristics bands
PET	Biomass	Pellets	
-	3,324	3,340	Hydroxyl (O-H) groups
2,916	-	2,960	C–H stretching in aromatic methoxyl groups and methylene groups
-	2,898	-	C-H stretching in the methyl groups
-	1,734	-	Stretching of C=O of the carbonyl, carboxyl, and acetyl groups, and of xylans
1,714	-	1,713	The non-conjugated carbonyl group stretching
-	1,593	1,578	Aromatic skeleton vibration (C=C) of lignin
-	1,442	-	C-H deformation in lignin and carbohydrates, CH_2 stretching, and CH_3 asystematic
1,338-1,408	-	1,337-1,408	Stretching of C-O group deformation of the O-H group and bending and wagging vibrational modes of the ethylene glycol segment
1,247&1,125	-	1,252-1,239	Terephthalate group ($OOCC_6H_4$-COO)
-	1,231		C-C, C-O, and C=O stretching
1,090	-	1,083	Si-O asymmetric
-	1,026	1,022	Stretching of C-O of the ester-methyl group of lignin
950-1,016	-	1,016	Si-O(H) asymmetric
796	-	723	Si-O symmetric
-	559	-	C-H bending
439	-	459	Si-O-Si bending

a band at 3,324/cm (O-H group) due to the water content in the biomass sample. In addition, there were bands at 2,898/cm (C-H stretch), 1,734/cm (C=O, stretch), 1,593/cm (C=C, aromatic skeleton vibration), 1,442/cm (C-H, CH_2, stretch, and CH_3, asystematic), 1,231/cm (C-C, C-O, and C=O, stretch), 1,026/cm (C-O, stretch), and 559/cm (C-H, bend). Similar results for the functional groups of lignocellulosic materials have been reported using FTIR in teak hardwood, coffee grounds, and sugarcane bagasse (Lopes *et al.,* 2018; Manatura, 2020; Taleb *et al.,* 2020). The PET/biomass pellets characterization interpreted the mixture between PET waste and biomass as seen in Fig. 2c. While functional groups were contributed by both raw materials, the mixture was mainly characterized by the functional groups from the PET waste at around 1,252-1,239/cm, represented groups of terephthalate. Even though the biomass made up a small proportion of the pellets, some biomass characteristics were evident in the band at 1,578/cm that showed vibration of the aromatic skeleton with stretching (C=C) of lignin and at 1,022/cm representing C-O stretching of the ester methyl group of lignin. However, silica group occurred bands at 1,016, 723, and 459/cm in the sample of PET/biomass pellets due to the contamination was resulted from earth materials as found in the sample of PET waste.

Heavy metal concentration and ionic leachability

Table 3 summarizes the results of heavy metal concentration and ionic contaminants of the raw materials and PET/biomass pellets. The concentrations of Pb, Zn, Cr, and Cu in all tests of raw material samples were below regulatory levels and none of the tests yielded evidence of Cd. These results confirmed that the heavy metals (Cd~Cu<Pb<Cr<Zn) content in PET/biomass pellets were below the limits set by some European countries (Finland, Italy, France and the Netherlands) for alternative solid fuels such as RDF and SRF (Zhao *et al.,* 2016). In addition, the contaminant leaching of AnL and CaL was also investigated and reported in Table 4. The PET waste had a high content of chloride (Cl^-) of around 3.99 ppm and the other six tested anions were recorded in the range from non-detectable to 0.33 ppm, while for the cations, sodium (Na^+) was the highest (28.35 ppm). The biomass sample had a substantially amount of the phosphate (PO_4^{3-}) anion at 58.58 ppm with lesser amounts of the other three cations-potassium (K^+) at 28.57 ppm, sodium (Na^+) at 16.21 ppm, and magnesium (Mg^{2+}) at 7.42 ppm. The experimental results showed that pellets characterization regarding ionic leachability was based on the combined properties of the PET waste and biomass. The major ionic elements in

the pellets were not higher than in the original biomass for PO_4^{3-}, Cl^-, F^-, SO_4^{2-}, K^+, Mg^{2+}, and Ca^{2+} and furthermore, were not higher than in the PET waste for Cl^- and Na^+. The high sodium (Na^+) cation level in the PET waste and the pellets might have been affected by the caustic soda (NaOH) detergent used during the cleaning step in the mechanical recycling process for the PET bottles.

Ash composition

The ash composition analysis obtained by EDXRF technique showed in Table 5. The ashes from combustion of biomass, PET, and PET/biomass pellets would consist of the most common oxides which formed during the sintering process (Lu *et al.*, 2015). Silicon oxide (SiO_2), iron (III) oxide (Fe_2O_3), calcium oxide (CaO), magnesium oxide (MgO), and aluminium oxide (Al_2O_3) were the major components of all ash samples. The content of SiO_2 in biomass ash was 48.88%wt or more suggested by Xing *et al.* (2016) for the raw materials of biomass, which was much lower than PET (78.24%wt) and pellets (80.68%wt). While the lower SiO_2 (10.32%wt) composition of waste from PET bottles washing has been reported by Jabłońska *et al.* (2019). SiO_2 composition occurred in the samples of waste PET and PET/biomass pellets due to the contamination was mainly resulted from earth materials. The biomass ash had a substantially amount of phosphorus (V) oxide (P_2O_5), and potassium oxide (K_2O) were 6.14% and 4.23%, respectively. Chromium (III) oxide (Cr_2O_3), copper oxide (CuO), zinc oxide (ZnO), titanium dioxide (TiO_2) were found in the ash of pellets sample. These metal-oxides fractions in the ash were supposed the effect of aggregation of metal elements with oxygen during combustion process (Samaksaman *et al.*, 2015). The appearance of metal elements such as CrO, CuO, ZnO, and TiO_2 might be released during the process of PET-bottle grinding and PET/biomass pelletizing. Sulfur trioxide (SO_3) was also found in the low value. Trace metals such as manganese (IV) oxide (MnO_2), strontium oxide (SrO), zirconium dioxide (ZrO_2), and tantalum (V) oxide

Table 3: The results of heavy metal concentration

Sample	Heavy metal concentration (mg/kg)				
	Pb	Zn	Cd	Cr	Cu
Limits [a]	200	500	5	100	300
PET	ND	3.5	ND	9.4	5.0
Biomass	ND	0.7	ND	1.6	1.4
Pellets	0.8	7.4	ND	5.2	ND

[a] The limits set by European countries for the RDF and SRF.
ND: not detected

Table 4: The results of anionic and cationic leachability

Sample	AnL (ppm)							CaL (ppm)					
	F^-	Cl^-	NO_2^-	Br^-	NO_3^-	PO_4^{3-}	SO_4^{2-}	Li^+	Na^+	NH_4^+	K^+	Mg^{2+}	Ca^{2+}
PET	0.06	3.99	ND	ND	ND	ND	0.33	ND	28.35	ND	0.55	1.52	1.82
Biomass	0.32	4.61	ND	ND	ND	58.58	1.75	ND	16.21	ND	28.57	7.42	3.88
Pellets	0.06	3.25	ND	ND	ND	16.96	0.62	ND	20.88	ND	10.70	2.71	2.03

AnL: Anions leachate; CaL: Cations leachate; ND: not detected

Table 5: Composition of the different ash samples

Sample	Ash composition (%wt)															
	MgO	Al_2O_3	SiO_2	P_2O_5	SO_3	K_2O	CaO	TiO_2	Cr_2O_3	MnO_2	Fe_2O_3	CuO	ZnO	SrO	ZrO_2	Ta_2O_5
PET	3.29	4.23	78.24	0.15	0.27	0.75	3.93	0.95	0.08	0.10	7.88	0.05	0.04	ND	0.03	ND
Biomass	9.21	10.02	48.88	6.14	0.64	4.23	16.08	0.49	0.06	0.08	4.11	0.01	0.01	0.02	0.01	0.01
Pellets	2.86	2.63	80.68	1.27	0.13	0.65	3.80	0.53	0.45	ND	6.94	0.03	0.03	ND	ND	ND

ND: not detected

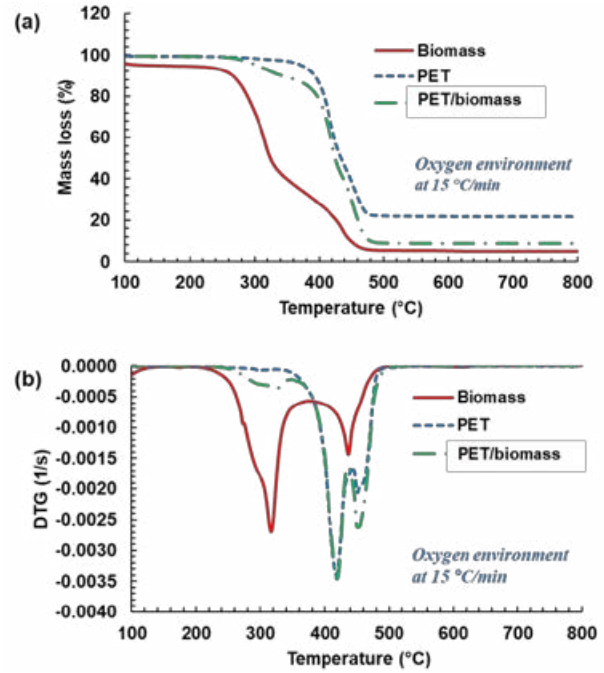


Fig. 3: (a) TGA and (b) DTG for combustion of waste of PET (PET), biomass (Biomass), and pellets (PET/biomass) at 15 °C/min

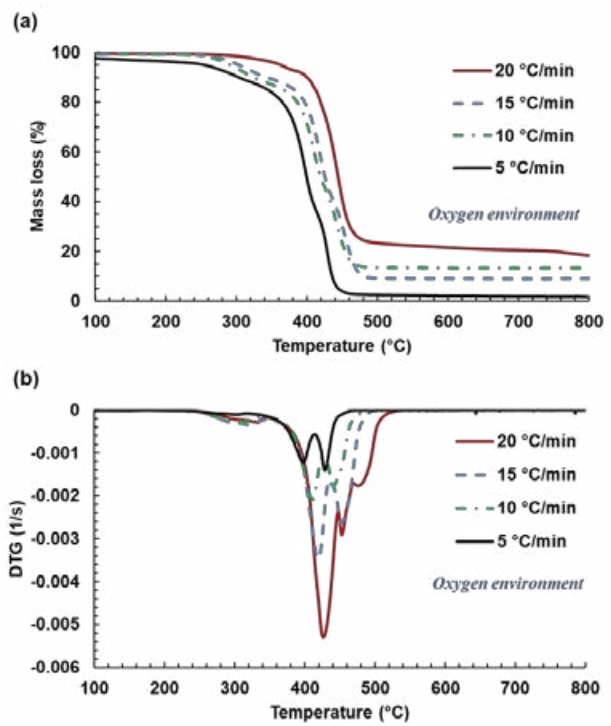


Fig. 4: (a) TGA and (b) DTG for combustion of pellets at 5-20 °C/min

(Ta_2O_5) were untraceable in the ash of pellets sample. It is proven that the ash characterization of pellets exhibited unique characters based on the combined properties of the PET waste and biomass. Overall, the results of properties and fuel characteristics, FTIR, heavy metal concentration and ionic leachability, and ash composition made the PET/biomass pellets useful in a co-firing process with traditional solid fuels. Moreover, the PET/biomass pellets can further be upgraded to other fuels production via modern bioenergy conversion processes.

TGA and DTG results

The combustion characteristics of PET waste and the raw biomass at 15 °C/min are shown in the TG and DTG curves in Fig. 3. Both waste of PET and biomass are different in chemical structure, but the tests could be compared because used the same condition of oxygen atmosphere and a heating rate. The reaction temperature varied in the range 100 to 800 °C. It was clear that the biomass characteristics differed noticeably compared to those of the PET. For the biomass, below 150 °C represented removing vapor and light volatile matter (Ahmad *et al.,* 2017). The mass loss of about 5.80% was represented as the water content in biomass (Fig. 3a). The clear mass loss of the biomass commenced from 190 up to 500 °C. Two clear peaks were observed during combustion with maximum mass loss rates of 0.0027 s^{-1} at 317 °C and 0.0014 s^{-1} at 437 °C, respectively. The first and second peaks were caused by the release of volatile matter in the temperature range from 148 to 372 °C and combustion of the remaining char, respectively (Ahn *et al.,* 2014). For all samples of the PET waste and PET/biomass pellets, no obvious mass loss was detected below 266 °C. However, a small peak was observed with 0.0003 s^{-1} at 325 °C for the mixed PET with biomass related to the level of higher volatiles in the biomass. The distinct mass loss and rate of mass loss of the PET waste and the pellets started at 278 °C and finished at around 458 °C. Two peaks were observed in Fig. 3b, with the first peak being for PET waste and pellets that were very similar to each other with a maximum mass loss rate of 0.0034 s^{-1} at 419 °C. The second peak had the same peak temperature (T_p) at 454 °C with the mass loss rate for pellets of 0.0026 s^{-1} and for PET waste of 0.0020 s^{-1}, respectively. It was clear that the biomass blending supported reactivity of the process. In addition, the experimental results affirmed that the decomposition of material with complex structure depended on the loss of chemical bonding and properties of materials. The combustion properties of the PET waste, biomass, and pellets are listed in Table 6. The ignition temperature (T_{ig}) and peak temperature (T_p) of PET were consistent with Das and Tiwari (2019). The results indicated that a low content (10%wt) of biomass mixed with PET improved T_{ig} by lowering it. There were no obvious changes in other properties such as the burnout temperature (T_b), higher reactivity (R_{avg}), and maximum derivative thermogravimetric value (DTG_{max}). The effects of the heating rate (5, 10, 15 and 20 °C/min) on mass loss and the rate of mass loss in terms of combustion temperature are shown in Fig. 4. The mass loss and rate of mass loss curves

Table 6: Thermal decomposition of samples in combustion at 15 °C/min

Sample	T_{ig} (°C)	T_b (°C)	T_p (°C)	DTG_{max} (1/s)	R_{avg} (1/(s·K))
PET	390	475	419	-0.0034	-4.92E-06
Biomass	278	458	317	-0.0027	-4.56E-06
Pellets	380	471	420	-0.0035	-4.99E-06

Table 7: Combustion characteristics of pellets in combustion at various heating rates

Hearing rate (°C/min)	T_{ig} (°C)	T_b (°C)	T_p (°C)	DTG_{max} (1/s)
5	360	460	398	-0.0012
10	378	460	411	-0.0021
15	380	471	420	-0.0035
20	398	499	426	-0.0053

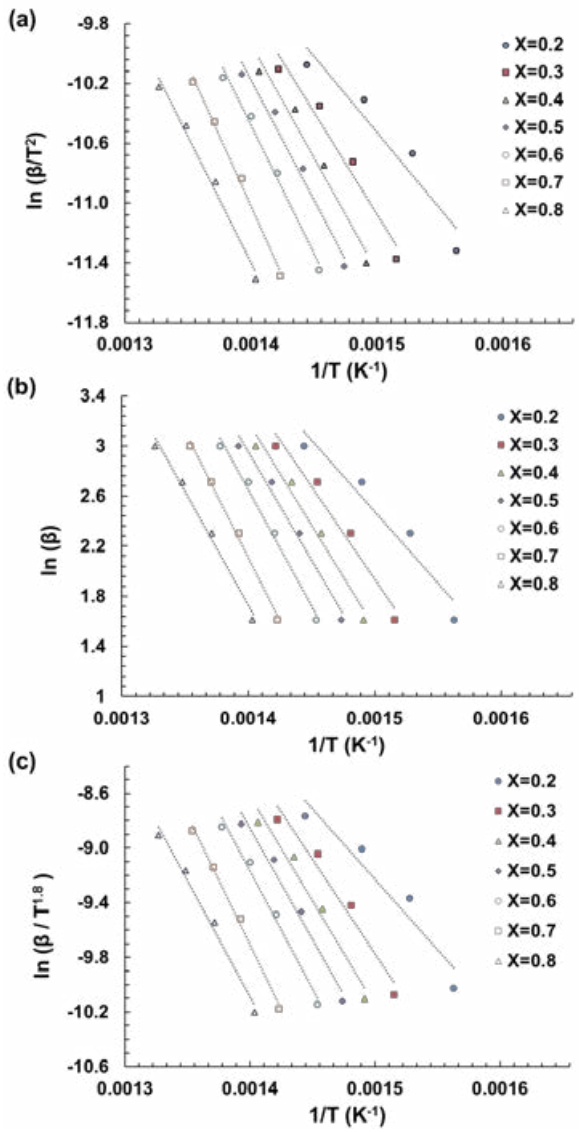


Fig. 5: Linear regression lines; (a) KAS, (b) OFW, and (c) Starink at various conversions (X)

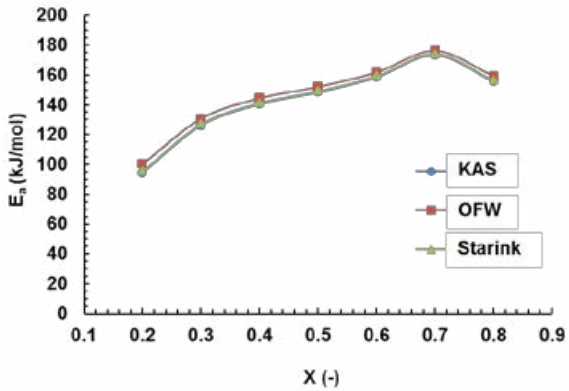


Fig. 6: E_a vs X for the KAS, OFW, and Starink

were parallel and similar. A higher heating rate required a larger temperature range for complete combustion because there was not sufficient time for the biomass to combust (Manatura *et al.,* 2018). Table 7 shows the combustion characteristics of pellets for the four heating rates. With an increased heating rate, the values of T_{ig}, T_b, and T_p increased as did DTG_{max}, indicating that the lower heating rate produced more effective combustion than the higher heating rate (Lu and Chen, 2015).

Kinetic analysis

The iso-conversional KAS, OFW and Starink methods from Eq. (9)-(11) were used to determine the kinetic factors (E_a and A) in this study. The typical linear regression lines of the KAS, OFW, and Starink methods fitted with conversion (X) in the range 0.2 to 0.8 are shown in Fig. 5. The estimates of E_a and A from the models were very close in value, as shown in Table 8. The quality of linear fitting is shown by R^2, with the values being mostly higher than 0.96 which implied the simulations had a good fit with the experimental data. Fig. 6 illustrates the variation of E_a in terms of X. The kinetic factors E_a and A showed similar trends by increasing first for X values of 0.2 to 0.7, then decreasing at 0.8. The minimum and maximum E_a values were at X values of 0.2 and 0.7, respectively. It was noticed that a rapid increase in E_a occurred between X values in the range 0.6-0.7 because almost all the volatile matter was expelled from the char residue. Moreover, E_a rapidly dropped for X values in the range 0.7-0.8 due to the sudden char combustion at the higher temperature in the oxygenated atmosphere (Das and Tiwari, 2019). The average E_a value for pellets was in the range 142 to 146 kJ/mol for all prediction models, with these values in accordance with previous work of Das and Tiwari (2019), as was the average value of A represented in the range 6.70×10^{12} to 1.83×10^{15} min^{-1}.

Thermodynamic parameters

To design a high performance macro-scale combustor requires not only choosing suitable bio-fuels and kinetic parameters but also requires

Table 8: Thermokinetic factors of pellets for three models

X (-)	KAS			OFW			Starink		
	E_a (kJ/mol)	A (min^{-1})	R^2 (-)	E_a (kJ/mol)	A (min^{-1})	R^2 (-)	E_a (kJ/mol)	A (min^{-1})	R^2 (-)
0.2	94.31	2.76E+07	0.92	100.16	8.21E+09	0.93	95.06	7.48E+09	0.92
0.3	126.15	1.07E+10	0.96	130.65	1.90E+12	0.97	126.80	2.91E+12	0.96
0.4	140.41	1.53E+11	0.97	144.34	2.26E+13	0.97	141.03	4.15E+13	0.97
0.5	148.37	6.66E+11	0.98	152.01	9.02E+13	0.98	148.97	1.81E+14	0.98
0.6	158.46	3.83E+12	0.99	161.72	4.66E+14	0.99	159.04	1.04E+15	0.99
0.7	173.42	4.06E+13	1.00	176.14	4.29E+15	1.00	173.97	1.11E+16	1.00
0.8	155.58	1.62E+12	0.99	159.35	2.17E+14	0.99	156.21	4.44E+14	0.99
Avg.	142.38	6.70E+12	-	146.34	7.26E+14	-	143.01	1.83E+15	-

Table 9: Thermodynamic analysis of pellets at 15 °C/min

X (-)	A (s^{-1})	ΔH (kJ/mol)	ΔG (kJ/mol)	ΔS (J/mol·K)
0.2	7.63E+04	88.73	204.07	-166.50
0.3	2.57E+07	120.45	202.40	-118.29
0.4	3.40E+08	135.09	201.78	-96.27
0.5	1.43E+09	142.55	201.46	-85.05
0.6	8.82E+09	152.56	201.08	-70.04
0.7	1.30E+11	167.41	200.56	-47.85
0.8	5.25E+09	149.48	201.19	-74.64
Avg.	2.08E+10	136.61	201.79	-94.09

investigating the thermodynamic parameters (Xu and Chen, 2013). Thermodynamic factors such as A, ΔH, ΔG, and ΔS evaluated using the OFW method under the TGA conditions of a heating rate at 15 °C/min, are shown in Table 9. The A value increased from 7.63×10^4 to 1.30×10^{11} for X values in the range from 0.2 to 0.7, respectively, and then decreased to 5.25×10^9 at an X value of 0.8. The lowest and highest values of A were 7.63×10^4 and 1.30×10^{11} at X values of 0.2 and 0.7, respectively. The higher values of A were due to elevated numbers of molecular collisions so more heat was generated which was related to the values of E_a (Fong et al., 2019). On the other hand, the lowest A indicated a restriction in particle rotation of the activated complex compared to the initial reagent, indicating a large surface reaction (Zhang *et al.,* 2016). ΔH is the deviation of energy between the reagent and the activated complex depending on the activation energy (Xu and Chen, 2013). ΔH increased from 88.73 to 167.41 kJ/mol and decreased to 149.48 kJ/mol with an average of 136.61 kJ/mol during the conversion. It was noticed that the deviation between E_a and ΔH was very low (about 10 kJ/mol) which implied that this reaction was simple to achieve product formation (Ahmad *et al.,* 2017). Positive values of ΔH represent an endothermic reaction which requires an external heat source to break and form new chemical bonds. The ΔG value refers to the amount of available energy for the formation of activated complexes (Laougé and Merdun, 2020). It was quite steady for X values from 0.2 to 0.8 with an average ΔG of 201.79 kJ/mol which was consistent with Das and Tiwari (2019). This indicated that the combustion of the mixed PET waste with biomass consumed more energy compared to chicken manure (163.37-165.39 kJ/mol) (Yuan *et al.,* 2017). The high ΔG value showed that the PET/biomass pellets were an optimal choice for converting the PET waste and biomass to energy. The values of E_a, ΔH, and A were the highest at an X value of 0.8 for combustion. The ΔS value measures the disorder or randomness of energy and matter in

a system and shows how near of far the state of the sample is from its own thermodynamic equilibrium. Entropy also shows the degree of arrangement of the carbon layers in samples (Xu and Chen, 2013). Positive values indicate a high affinity of the sorbent and negative values indicate that the adsorption process is mainly driven by ΔS. In the current study, the ΔS values were negative regardless of the model and process used. The higher values of ΔS occurred between X values of 0.2 and 0.3 (-166.50 and -118.29 J/(mol.K)), respectively. It was observed that the trend for ΔS was opposite that of E_a, ΔH, and ΔG.

CONCLUSION

Increase in fuel pellets demand coupled with rising environmental issues of the secondary waste from the plastic recycling system have attracted researcher to explore. Fuel pellets production by pelletizing is an efficient method for manipulating waste of PET from a mechanical recycling plant and local biomass like teak sawdust. It is a useful tool to manage the waste of PET and biomass in terms of dusty forms (macro-, meso-, micro-, and nano-sizes) and plays a role on reduce the loads of plastic waste pollution that releases into the soil, public water, as well as air emissions. Notice, the reduction of loads of plastic waste dumps into landfills and to prevent the improper disposal of plastic waste are considered. In further, it can adapt into a concept of waste to energy following by converting to fuel pellets and using with industrial furnaces i.e. using as substituent fuels in cement kiln, boiler, power plant, incinerator, and so on. Pelletizing was employed to convert waste of PET and biomass into a potential solid fuel with the fit ratio of 9:1 (PET:biomass). This ratio gives the durability of PET/biomass pellets, a uniform dimension, ease handling, storage, and transportation common as woody pellets. Some technical challenges such as low moisture content and high volatile matter content were feedstock dependent. The PET/biomass pellets had characteristics and physico-chemical properties that were a combination of those of the PET waste and biomass. A high heating value of the PET/biomass pellets (HHV = 19.20 MJ/kg) was obtained from the results of pelletizing the complex solid fuels. The HHV value was slightly decreased by adding biomass. The complex structure of ethylene terephthalate and lignocellulose was clearly identified by FTIR technique. Heavy metals (Cd~Cu<Pb<Cr<Zn) and ionic (7 AnLs and 6 CaLs) contaminants had lower concentration than the limitation of the regulations. The results of ash composition affirmed that the ash of PET/biomass pellets was a non-hazardous residue which was unique characters based on feedstock. Therefore, the PET/biomass pellets can be used without harms of the environment and health impacts. Earth materials (SiO_2 composition) and a detergent (Na^+ element of caustic soda) from step PET flake cleaning had a slightly effect on the alteration of residue chemicals. However, biomass supplied as part of PET plastic waste improve combustion kinetics such as T_{ig}, T_b, R_{avg}, and DTG_{max}. Lower ignition temperature, burnout temperature, reactivity, and DTG_{max} were affected by the blended biomass in the PET/biomass pellets that could be attributed to the combined effect of terephthalate and lignocellulose groups present in the pellet matrix. Subsequently, the combustion characteristics and kinetics of PET/biomass pellet samples were examined via the iso-conversional methods of KAS, OFW, and Starink. The results exhibited similar trends and values for the activation energy (E_a) of 142.38, 146.34, and 143.01 kJ/mol, respectively, with the values of conversion ranged from 0.2 to 0.8. The thermodynamic factors of ΔH, ΔG, and ΔS were 136.61 kJ/mol, 201.79 kJ/mol, and -94.09 J/mol×K, respectively. These findings may provide comprehensive knowledge to assist the design and operation of a combustion system for adding PET/biomass pellets in a co-firing process with traditional solid fuels. Moreover, PET/biomass pellets can further be upgraded to other fuels production via modern bioenergy conversion processes.

AUTHOR CONTRIBUTIONS

K. Manatura performed the literature review, writing original draft, conceptualization, methodology, investigation, data analysis, visualization, and manuscript edition. U. Samaksaman performed the literature review, experimental design, analyzed and interpreted the data, research summary and recommendation, and manuscript edition.

ACKNOWLEDGEMENT

This study was supported by grants from the Faculty of Engineering at Kamphaeng Saen, Kasetsart University, Kamphaeng Saen campus, Thailand [Project No. 10/2020] and Naresuan University, Thailand (R2560C032). The authors also thank the

Kasetsart University Research and Development Institute (KURDI), Bangkok, Thailand for English-editing assistance.

CONFLICT OF INTEREST

The authors declare no potential conflict of interest regarding the publication of this work. In addition, the ethical issues including plagiarism, informed consent, misconduct, data fabrication and, or falsification, double publication and, or submission, and redundancy have been completely witnessed by the authors.

ABBREVIATIONS

%	Percentage
% wt	Weight percentage
°C	Degrees celsius
°C/min	Heating rate (degree of temperature per time)
ΔG	Gibbs free energy
ΔH	Enthalpy
ΔS	Entropy
A	The pre-exponential factor
Al_2O_3	Aluminium oxide
AnL	Anions leachate
β	The heating rate varies with the reaction time and temperature at a constant heating rate
Br^-	Bromide
cm	Centimeter
1/cm	The unit of wavenumber of IR spectrum
C	Carbon
CaL	Cations leachate
CaO	Calcium oxide
Ca^{2+}	Calcium
Cd	Cadmium
Cl^-	Chloride
Cr	Chromium
Cr_2O_3	Chromium (III) oxide
Cu	Copper
CuO	Copper oxide
CEN/TS 15148	Method for the determination of the content of volatile matter
CEN/TS 14775	Method for the determination of ash content
DI water	The deionized water
DTG	Derivative thermogravimetry
DTG_{max}	Maximum derivative thermogravimetric value (1/s)
E_a	The activation energy (kJ/mol)
Eq.	Equation
EDXRF	Energy dispersive X-ray fluorescence spectroscopy
f(x)	The reaction model expressing the dependence of the combustion rate
F^-	Fluoride
FC	Fixed carbon
Fe_2O_3	Iron (III) oxide
FTIR	Fourier transform infrared spectrometry
g(X)	The integral form of *f(X)*
h	Plank constant $6{\cdot}626 \times 10^{-34}$ (J·s)
H	Hydrogen
HDPE	High density polyethylene
HHV	High heating value
H/C	Hydrogen to carbon atomic ratio
IR	Infrared radiation
k	The combustion rate constant
kg/min	Kilogram per minute
kV	Kilovoltage
K	Degrees Kelvin
K^+	Potassium
K_B	The Boltzmann constant $1{\cdot}381 \times 10^{-23}$ (J/K)
KAS	The Kissinger-Akahira-Sunose method
K_2O	Potassium oxide
Li^+	Lithium
mg/kg	Miligram per kilogram
ml	Milliliter
mm	Millimeter
mΩ	Milliohm
min^{-1}.	The unit of A interm of minute (pre-exponential factor)
m_0	The initial sample mass

m_f	The sample mass left after ending process
m_t	The sample mass at time *t*
MC	Moisture content
MJ/kg	Megajoules per kilogram
MgO	Magnesium oxide
Mg^{2+}	Magnesium
MnO_2	Manganese (IV) oxide
N	Nitrogen
Na^+	Sodium
NaOH	Sodium hydroxide (caustic soda)
NH_4^+	Ammonium
NO_x	Oxides of nitrogen
NO_2^-	Nitrite
NO_3^-	Nitrate
O	Oxygen
OFW	The Ozawa-Flynn-Wall method
O/C	Oxygen to carbon atomic ratio
ppm	Part per million
Pb	Lead
PET	Polyethylene terephthalate
PET/ biomass	The mixture of PET and biomass
PO_4^{3-}	Phosphate
PP	Polypropylene
P_2O_5	Phosphorus(V) oxide
R	The universal gas constant 8.314 (kJ/(kmol·K))
R^2	The coefficient of determination value
R_{avg}	Higher reactivity
RDF	Refuse derived fuel
Rh X-ray	Rhodium X-ray tube
s^{-1}	The unit of A interm of second (pre-exponential factor)
S	Sulfur
SiO_2	Silicon oxide
SO_2	Sulfurdioxide
SO_3	Sulfur trioxide
SO_4^{2-}	Sulfate
SrO	Strontium oxide
SRF	Solid recovered fuel
Starink	The Starink method
T	The absolute temperature (K)
Ta_2O_5	Tantalum (V) oxide
TiO_2	Titanium dioxide
T_b	Burnout temperature
T_{ig}	Ignition temperature
T_p	Peak temperature
TGA	Thermogravimetric analysis
v/v	The volume ratio
VM	Volatile matter
X	The conversion of samples
XRF	X-ray fluorescence spectroscopy
XGT diameter	The X-ray irradiation diameter
Zn	Zinc
ZnO	Zinc oxide
ZrO_2	Zirconium dioxide

REFERENCES

Abnisa, F.; Wan Daud, W., (2014). A review on co-pyrolysis of biomass: An optional technique to obtain a high-grade pyrolysis oil. Energy Convers. Manage. 87: 71-85 **(15 pages).**

Ahmad, M.; Mehmood, M.; Ye, G.; Al-Ayed, O.; Ibrahim, M.; Rashid, U.; Luo, H.; Qadir, G.; Nehdi, I., (2017). Thermogravimetric analyses revealed the bioenergy potential of *Eulaliopsis binata*. J. Therm. Anal. Calorim. 130: 1237-1247 **(11 pages).**

Ahn, S.; Choi, G.; Kim, D., (2014). The effect of wood biomass blending with pulverized coal on combustion characteristics under oxy-fuel condition. Biomass. Bioenerg. 71: 144-154 **(11 pages).**

Akahira, T.; Sunose, T., (1971). Method of determining activation deterioration constant of electrical insulating materials. Res. Rep. Chiba. Inst. Technol. (Sci. Technol.) 16: 22-31 **(10 pages).**

Basu, P.; Butler, J.; Leon, M., (2011). Biomass co-firing options on the emission reduction and electricity generation costs in coal-fired power plants. Renew. Energy 36: 282-288 **(7 pages).**

Beata, J.; Paweł, K.; Maroš, K.; Tomasz, D., (2019). Physical and chemical properties of waste from PET bottles washing as a component of solid fuels. Energa. 12: 1-17 **(17 pages).**

Becidan, M.; Várhegyi, G.; Hustad, J.; Skreiberg, Ø., (2007). Thermal decomposition of biomass wastes. A kinetic study. Ind. Eng. Chem. Res. 46(8): 2428-2437 **(10 pages).**

Block, C.; Ephraim, A.; Weiss-Hortala, E.; Minh, D.; Nzihou, A.; Vandecasteele, C., (2019). Co-pyrogasification of Plastics and Biomass, a Review. Waste Biomass Valorization. 10: 483-509 **(17 pages).**

Bu, Q.; Liu, Y,; Liang, J,; Morgan, H.; Yan, L.; Xu, F.; Mao, H., (2018). Microwave-assisted co-pyrolysis of microwave torrefied biomass with waste plastics using ZSM-5 as a catalyst for high quality bio-

oil. J. Anal. Appl. Pyrol. 134: 536-543 **(8 pages).**

Capeletti, L.; Zimnoch, J., (2016). Fourier Transform Infrared and Raman Characterization of Silica-Based Materials.

Çepelioğullar, Ö.; Pütün, A., (2013). Thermal and kinetic behaviors of biomass and plastic wastes in co-pyrolysis. Energy Convers. Manage. 75: 263-270 **(8 pages).**

Chandrasekaran, A.; Ramachandran, S.; Subbiah, S., (2017). Determination of kinetic parameters in the pyrolysis operation and thermal behavior of Prosopis juliflora using thermogravimetric analysis. Bioresour. Technol. 233: 413-422 **(10 pages).**

Chattopadhyay, J.; Kim, C.; Kim, R.; Pak, D., (2008). Thermogravimetric characteristics and kinetic study of biomass co-pyrolysis with plastics. Korean J. Chem. Eng. 25(5): 1047-1053 **(7 pages).**

Chen, L.; Wang, S.; Meng, H.; Wu, Z.; Zhao, J., (2017). Synergistic effect on thermal behavior and char morphology analysis during co-pyrolysis of paulownia wood blended with different plastics waste. Appl. Therm. Eng. 111: 834-846 **(14 pages).**

Chen, Z.; Hay, J.; Jenkins, M., (2013). The thermal analysis of poly(ethylene terephthalate) by FTIR spectroscopy. Thermochim. Acta 552: 123-130 **(8 pages).**

Das, P.; Tiwari, P., (2019). Thermal degradation study of waste polyethylene terephthalate (PET) under inert and oxidative environments. Thermochim. Acta. 654: 191–202 **(12 pages).**

Edo, M.; Budarin, V.; Aracil, I.; Persson, P.; Jansson, S., (2016). The combined effect of plastics and food waste accelerates the thermal decomposition of refuse-derived fuels and fuel blends. Fuel 180: 424-432 **(9 pages).**

Fong, M.; Loy, A.; Chin, B.; Lam, M.; Yusup, S.; Jawad, Z., (2019). Catalytic pyrolysis of *Chlorella vulgaris*: Kinetic and thermodynamic analysis. Bioresour. Technol. 289: 121689.

Gai, C.; Dong, Y.; Zhang, T., (2013). The kinetic analysis of the pyrolysis of agricultural residue under non-isothermal conditions. Bioresour. Technol. 127: 298-305 **(8 pages).**

Govindan, B.; Jakka, S.; Radhakrishnan, T,; Tiwari, A.; Sudhakar, T.; Shanmugavelu, P.; Kalburgi, A.; Sanyal, A.; Sarkar, S., (2018). Investigation on kinetic parameters of combustion and oxy-combustion of calcined pet coke employing thermogravimetric analysis coupled to artificial neural network modeling. Energy Fuels 32(3): 3995-4007 **(13 pages).**

Huang, Y.; Lo, S., (2020). Predicting heating value of lignocellulosic biomass based on elemental analysis. Energy 191: 116501.

Jabłońska, B.; Kiełbasa, P.; Korenko, M.; Dróżdż, T., (2019). Physical and chemical properties of waste from PET bottles washing as a component of solid fuels. Energies. 12(11): 1-17 **(17 pages).**

Laougé, Z.; Merdun, H., (2020). Pyrolysis and combustion kinetics of *Sida cordifolia* L. using thermogravimetric analysis. Bioresour. Technol. 299: 122602.

Lopes, J.; Garcia, R.; Souza, N., (2018). Infrared spectroscopy of the surface of thermally-modified teak juvenile wood. Maderas, Cienc. Technol., 20(4): 737-746 **(10 pages).**

Lu, C.; Chen, J.; Chuang, K.; Wey, M., (2015). The different properties of lightweight aggregates with the fly ashes of fluidized-bed and mechanical incinerators. Constr. Build. Mater. 101(1): 380-388 **(9 pages).**

Lu, J.; Chen, W., (2015). Investigation on the ignition and burnout temperatures of bamboo and sugarcane bagasse by thermogravimetric analysis. Appl. Energy 160: 49-57 **(9 pages).**

Luo, J.; Li, Q.; Meng, A.; Long, Y.; Zhang, Y., (2018). Combustion characteristics of typical model components in solid waste on a macro-TGA. J. Therm. Anal. Calorim. 132: 553-562 **(10 pages).**

Madadian, E.; Crowe, C.; Lefsrud, M., (2017). Evaluation of composite fiber-plastics biomass clinkering under the gasification conditions. J. Clean. Prod. 164: 137-145 **(9 pages).**

Manatura, K., (2019). Napier grass pyrolysis: Kinetic and thermodynamics analysis. RMUTI J. Sci. Technol. 12(2): 1-13 **(13 pages).**

Manatura, K., (2020). Inert torrefaction of sugarcane bagasse to improve its fuel properties. Case Stud. Therm. Eng. 19: 1-9 **(9 pages).**

Manatura, K.; Lu, J.; Wu, K., (2018). Thermal decomposition and kinetic modeling of torrefied *Cryptomeria japonica* in a CO_2 environment. Biofuels 9: 693-703 **(11 pages).**

Martín-Gullón, I.; Esperanza, M.; Font, R., (2001). Kinetic model for the pyrolysis and combustion of poly-(ethylene terephthalate) (PET). J. Anal. Appl. Pyrol., 58-59: 635-650 **(16 pages).**

Mishra, R.; Sahoo, A.; Mohanty, K., (2019). Pyrolysis kinetics and synergistic effect in co-pyrolysis of Samanea saman seeds and polyethylene terephthalate using thermogravimetric analyser. Bioresour. Technol., 289: 121608.

Mostafa, M.; Hu, S.; Wang, Y.; Su, S.; Hu, X.; Elsayed, S.; Xiang, J., (2019). The significance of pelletization operating conditions: An analysis of physical and mechanical characteristics as well as energy consumption of biomass pellets. Renew. Sustain. Energy Rev., 105: 332-348 **(17 pages).**

Narobe, M.; Golob, J.; Klinar, D.; Francetič, V.; Likozar, B., (2014). Co-gasification of biomass and plastics: Pyrolysis kinetics studies, experiments on 100kW dual fluidized bed pilot plant and development of thermodynamic equilibrium model and balances. Bioresour. Technol., 162: 21-29 **(9 pages).**

Nussbaumer, T., (2003). Combustion and co-combustion of biomass: Fundamentals, technologies, and primary measures for emission reduction. Energy Fuels. 17: 1510-1521 **(12 pages).**

Patnaik, S.; Kumar, S.; Panda, A., (2020). Thermal degradation of eco-friendly alternative plastics: kinetics and thermodynamics analysis. Environ. Sci. Pollut. Res. Int., 27: 14991–15000 **(10 pages).**

Pereira, A.; da Silva, M.; Lima Júnior, É.; Paula, A.; Tommasini, F.; (2017). Processing and Characterization of PET Composites Reinforced With Geopolymer Concrete Waste. Mater. Res., 20(2): 411-420 **(10 pages).**

Pradhan, P.; Mahajani, S.; Arora, A., (2018). Production and utilization of fuel pellets from biomass: A review. Fuel Process. Technol., 181: 215-232 **(18 pages).**

Robinson, T.; Bronson, B.; Gogolek, P.; Mehrani, P., (2016). Comparison of the air-blown bubbling fluidized bed gasification of wood and wood–PET pellets. Fuel 178: 263-271 **(9 pages).**

Sajdak, M.; Kmieć, M.; Micek, B.; Hrabak, J., (2019). Determination of the optimal ratio of coal to biomass in the co-firing process: feed mixture properties. Int. J. Environ. Sci. Technol., 16: 2989-3000. **(12 pages).**

Samaksaman U.; Kuo J.; Peng T.; Wey M., (2015). Determination of emission characteristics during thermal treatment of lube oil and heavy metal co-contaminated soil by fluidized bed combustion, J. Environ. Eng., 141(10): 1-12 **(12 pages).**

Samaksaman, U.; Pattaraprakorn, W.; Neramittagapong, A.; Kanchanatip, E., (2021). Solid fuel production from macadamia

nut shell: effect of hydrothermal carbonization conditions on fuel characteristics. Biomass Conv. Bioref., 1-8 **(8 pages).**

Sharara, M.; Sadaka, S., (2014). Thermogravimetric analysis of swine manure solids obtained from farrowing, and growing-finishing farms. J. Sustain. Bioenergy Syst., 4(1): 75-86 **(12 pages).**

Sinha, V.; Patel, M.; Patel, J., (2010). PET waste management by chemical recycling: A review. J. Polym. Environ., 18: 8-25 **(18 pages).**

Slopiecka, K.; Bartocci, P.; Fantozzi, F., (2012). Thermogravimetric analysis and kinetic study of poplar wood pyrolysis. Appl. Energy 97: 491-497 **(7 pages).**

Surenderan, L.; Saad, J.; Zhou, H.; Neshaeimoghaddam, H.; Abdul Rahman, A., (2018). Characterization studies on waste plastics as a feedstock for energy recovery in Malaysia. Int. J. Eng. Technol., 7(4): 534-537 **(4 pages).**

Taleb, F.; Ammar, M.; Mosbah, M.; Salem, R.; Moussaoui, Y., (2020). Chemical modification of lignin derived from spent coffee grounds for methylene blue adsorption. Sci. Rep., 10: 11048 **(13 pages).**

Tolinski, M., (2011). Plastics and sustainability, towards a peaceful coexistence between bio-based and fossil fuel-based plastics, CH7, Processing: Increasing efficiency in the use of energy and materials. Scrivener Publishing, ISBN: 978-0-470-93878-2 **(19 pages).**

Tran, K.; Bach, Q.; Trinh, T.; Seisenbaeva, G., (2014). Non-isothermal pyrolysis of torrefied stump–A comparative kinetic evaluation. Appl. Energy. 136: 759-766 **(8 pages).**

Vyazovkin, S.; Wight, C., (1999). Model-free and model-fitting approaches to kinetic analysis of isothermal and nonisothermal data. Thermochim. Acta. 340-341: 53-68 **(16 pages).**

Wang, Z.; Burra, K.; Lei, T.; Gupta, A., (2021). Co-pyrolysis of waste plastic and solid biomass for synergistic production of biofuels and chemicals-A review. Prog. Energy Combust. Sci., 84: 1-51 **(51 pages).**

Xie, C.; Liu, J.; Buyukada, M.; Evrendilek, F.; Samaksaman, U.; Kuo, J.; Ozyurt, O., (2019). Parametric assessment of stochastic variability in co-combustion of textile dyeing sludge and shaddock peel. Waste Manage., 96: 128-135 **(8 pages).**

Xing, P.; Mason, P.; Chilton, S.; Lloyd, S.; Jones, J.; Williams, A.; Nimmo, W.; Pourkashanian, M., (2016). A comparative assessment of biomass ash preparation methods using X-ray fluorescence and wet chemical analysis. Fuel. 182: 161-165 **(5 pages).**

Xu, Y.; Chen, B., (2013). Investigation of thermodynamic parameters in the pyrolysis conversion of biomass and manure to biochars using thermogravimetric analysis. Bioresour. Technol., 146: 485-493 **(5 pages).**

Yuan, X.; He, T.; Cao, H.; Yuan, Q., (2017). Cattle manure pyrolysis process: kinetic and thermodynamic analysis with isoconversional methods. Renew. Energy. 107: 489-496 **(8 pages).**

Zhang, S.; Dong, Q.; Zhang, L.; Xiong, Y., (2016). Effects of water washing and torrefaction on the pyrolysis behavior and kinetics of rice husk through TGA and Py-GC/MS. Bioresour. Technol., 199: 352-361 **(10 pages).**

Zhao, L.; Giannis, A.; Lam, W.; Lin, S.; Yin, K.; Yuan, G.; Wang, J., (2016). Characterization of Singapore RDF resources and analysis of their heating value. Sustain. Environ. Res., 26: 51-54 **(4 pages).**

AUTHOR (S) BIOSKETCHES

Manatura, K., Ph.D., Assistant Professor, Department of Mechanical Engineering, Faculty of Engineering at Kamphaeng Saen, Kasetsart University, Kamphaeng Saen campus, Nakhonpatom, Thailand. Email: *kanitmana@gmail.com*

Samaksaman, U., Ph.D., Instructor, Department of Natural Resources and Environment, Faculty of Agriculture Natural Resources and Environment, Naresuan University, Phitsanulok, Thailand. Email: *ukrits@nu.ac.th*

COPYRIGHTS

©2021 The author(s). This is an open access article distributed under the terms of the Creative Commons Attribution (CC BY 4.0), which permits unrestricted use, distribution, and reproduction in any medium, as long as the original authors and source are cited. No permission is required from the authors or the publishers.

HOW TO CITE THIS ARTICLE

Manatura, K.; Samaksaman, U., (2021). Characteristics and combustion kinetics of fuel pellets composed of waste of polyethylene terephthalate and biomass. Global J. Environ. Sci. Manage., 7(4): 625-642.

DOI: 10.22034/gjesm.2021.04.09

url: https://www.gjesm.net/article_244128.html